Pergamon

Cement and Concrete Research 31 (2001) 1277–1283

CEMENT AND CONCRETE RESEARCH

Resistance of alkali-activated slag concrete to carbonation

T. Bakharev[a,*], J.G. Sanjayan[a], Y.-B. Cheng[b]

[a]*Department of Civil Engineering, Monash University, Clayton, Victoria 3800, Australia*
[b]*Department of Materials Engineering, Monash University, Clayton, Victoria 3800, Australia*

Received 26 June 2000; accepted 12 June 2001

Abstract

This paper presents an investigation into durability of alkali-activated slag (AAS) concrete exposed to carbonation. Two tests were used which simulated exposure of AAS concrete to carbonated solution and to atmosphere high in carbon dioxide. These tests involved immersion of the concrete in 0.352 M sodium bicarbonate solution, and exposure to atmosphere with 10–20% of CO_2 at 70% relative humidity. It was found that the resistance of AAS concrete to carbonation was lower than that of ordinary Portland cement (OPC) concrete, and AAS concrete had higher strength loss and depth of carbonation than OPC concrete in both tests.

Keywords: Ground-granulated blast-furnace slag; Alkali-activated cement; Durability; Carbonation

1. Introduction

Alkali-activated slag (AAS) concrete is being investigated as a construction material due to some advantages that arise from its use. The benefits include utilisation of industrial by-products in manufacturing of concrete, low energy consumption and reduced CO_2 emission associated with the use of slag. AAS concrete was also reported to have a superior durability in aggressive environments as compared to ordinary Portland cement (OPC) [1–4]. However, some investigations reported high carbonation rate in AAS concretes [2]. Carbonation reactions in C_3S and OPC pastes and OPC concrete were subjects of several studies [5–9], while carbonation reactions in AAS slag pastes and concretes have received much less attention. This paper presents the study of the durability of the AAS concrete produced using Australian slag when exposed to carbonation.

2. Experimental

2.1. Materials

The chemical composition of slag is shown in Table 1. The blast-furnace slag is a granulated product ground to fineness of about 460 m^2/kg, with the particle size range of 1–10 μm, and is neutral with the basicity coefficient K_b=(CaO + MgO)/(SiO_2 + Al_2O_3) equal to 0.93. The slag is supplied with 2% blended gypsum. The chemical composition and properties of OPC used in OPC concrete preparations are also detailed in Table 1.

AAS concrete was prepared using sodium silicate glass (PQ Australia, Sodium Silicate Solution grade D, wt. ratio $SiO_2/Na_2O = 2$, % $Na_2O = 14.7$, % $SiO_2 = 29.4$) and sodium hydroxide solutions (Ajax Chemicals, 60% w/v water solution) as activators. Liquid sodium silicate and sodium hydroxide were blended providing the modulus in solution (mass ratio of SiO_2 to Na_2O), M_s, equal to 0.75, and 4% Na in mixture with slag. Table 2 shows mix designs for concrete specimens. The AAS concrete had a nominal strength of 40 MPa at 28 days. The water-to-binder (w/b) ratio for AAS was fixed to 0.5 to enable direct comparison with OPC and reasonable concrete workability. OPC samples had a nominal compressive strength of 40 MPa at 28 days, and w/b = 0.5. Mixing of concrete was performed

* Corresponding author. 12 Terrigal Cl., N. Ringwood, Victoria 3134, Australia. Tel.: +61-3-9812-6795.
E-mail address: tbakharev@excite.com (T. Bakharev).

0008-8846/01/$ – see front matter
PII: S0008-8846(01)00574-9

Table 1
Composition of slag

Oxide (wt.%)	Slag[a]	Portland cement[b]
SiO_2	35.04	19.9
Al_2O_3	13.91	4.62
Fe_2O_3	0.29	3.97
CaO	39.43	64.27
MgO	6.13	1.73
K_2O	0.39	0.57
Na_2O	0.34	
TiO_2	0.42	
P_2O_5	<0.1	
MnO	0.43	
SO_3	2.43	2.56
Sulphide sulphur as S^{2-}	0.44	
Cl	80 ppm	
Loss on ignition	1.45	2.9
Bogue compounds (%)		
C_3S		64.2
C_2S		9.3
C_3A		5.7
C_4AF		12.2
Fineness (m^2/kg)	460	342

[a] SteelCement, Port Melbourne, Australia.
[b] Type I/II, Geelong, Victoria, Australia.

in a 70-l mixer. Activators were added in water. Initially, fine and coarse aggregates were premixed with small amount of water solution for 30 s. Then slag was added in the mix and the remaining water solution was gradually introduced and these constituents were mixed for 1.5 min. After a rest period of 2 min, mixing was resumed and continued for 2 min.

2.2. Test procedures

2.2.1. Carbonation

Since there is no accepted standard test for the carbonation of concrete, two kinds of carbonation tests were performed. The first test simulated concrete exposure to ground water containing high concentrations of carbonate ions and utilised 0.352 M solution of $NaHCO_3$ (referred to as carbonated water); the second test simulated carbonation in air and exposed the concrete to an atmosphere high in carbon dioxide. For the first test, the solution of $NaHCO_3$ was renewed after 1, 2, 6, 9, 12 months of exposure. The compressive strength and pH of concrete were monitored over 12 months. The products of degradation and microstructure were studied by X-ray diffraction (XRD) and scanning electron microscopy (SEM).

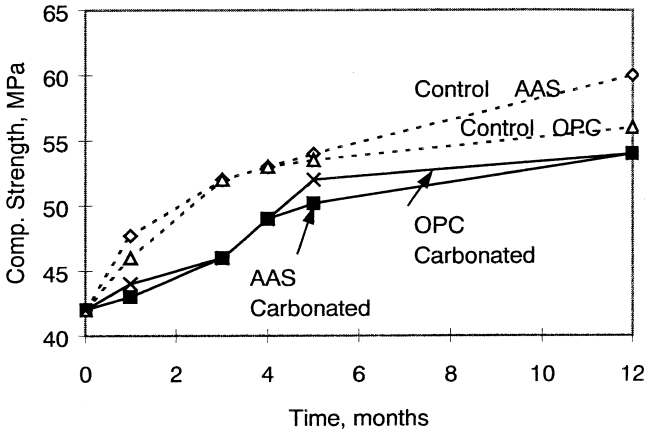

Fig. 1. Compressive strength of AAS and OPC concrete samples subjected to the 0.352-M solution of sodium bicarbonate. The dotted curves show the compressive strength of AAS and OPC samples cured in water.

Another test consisted in exposure of concrete to an atmosphere high in carbon dioxide gas. For the test, AAS and OPC concrete cylinders were stored in 20 l plastic drums (four cylinders per drum) with sealed lids in an atmosphere containing 10–20% CO_2 in air at 70% relative humidity for a period of 4 months. The volume of carbon dioxide introduced in the drum was measured using a constant flow valve and a timer. Every week, the atmosphere in the drum was renewed. Throughout 4 months, the compressive strength and pH of concrete were monitored.

A phenolphthalein method was used to monitor the pH of concrete in both experiments. In this method, phenolphthalein is used as an indicator of the pH change in the concrete pore solution. The usual method of studying carbonation is to measure the depth of neutralisation as indicated by a phenolphthalein solution, which has been sprayed onto the fractured concrete surface. This indicator shows a magenta-coloured region on the concrete where the pH value exceeds about 9 and a colourless region at the originally exposed surface where carbonation has reduced the pH to below 9 [9]. At the time of measurement, a 50% phenolphthalein solution in alcohol was sprayed on a surface of the concrete cylinder freshly cut using a large concrete saw, and with the

Table 2
Mix proportions of concretes (kg/m^3)

Mix description	Added water	Cementitious	Na-hydroxide solution	Na-silicate solution	Total water[a]	Coarse aggregates[b]	Fine aggregates[c]
AAS	147.4	Slag, 360	30.14	36.72	180	1130	830
OPC	180	Cement, 360	–	–	180	1130	830

[a] Total water includes added water and water in sodium silicate and sodium hydroxide solutions.
[b] Old basalt 14/10 mm (Pakhenham, Victoria).
[c] Concrete sand, FM = 2.18 (Lydhurst, Victoria).

orientation of the cylinder perpendicular to the longitudinal axis of symmetry.

2.2.2. Compressive strength

At predetermined intervals, the specimens were tested to find a strength reduction. Compressive strength testing was conducted on cylinders (∅100 × 200 mm). Prior to the compressive strength test, concrete cylinders were taken from the solution, dried, capped with a sulphur compound and tested. A total of three cylinders were tested for each data point. The companion specimens, cured in potable water, were also tested in compression. A reduction in compressive strength was calculated as follows:

$$\text{Reduction in compressive strength (\%)} = [(A-B)/A]\times 100\%,$$

where A = the average compressive strength of three specimens cured in water (MPa); and B = the average compressive strength of three specimens cured in the test solution (MPa).

2.2.3. X-ray diffraction

To perform XRD analysis, mortar was carefully removed from the surface region of a concrete sample subjected to the test. Each mortar sample was finely ground, and then analysed using XRD. XRD analyses were made using Rigaku Geigerflex D-max II automated diffractometer with the following conditions: 40 kV, 22.5 mA, Cu-Kα radiation. The XRD patterns were obtained by scanning at 0.1° (2θ) per min and in steps of 0.01° (2θ).

2.2.4. Scanning electron microscopy

Microstructures of samples exposed to tests were studied by an SEM (JEOL JSM-840 A) equipped with an EDS analyser (Oxford Image Analysis). The studies utilised backscattered electron imaging (BEI) of polished cross-section. Specimens were cut from the concrete and polished for examination of the surface and subsurface region for evidence of deterioration.

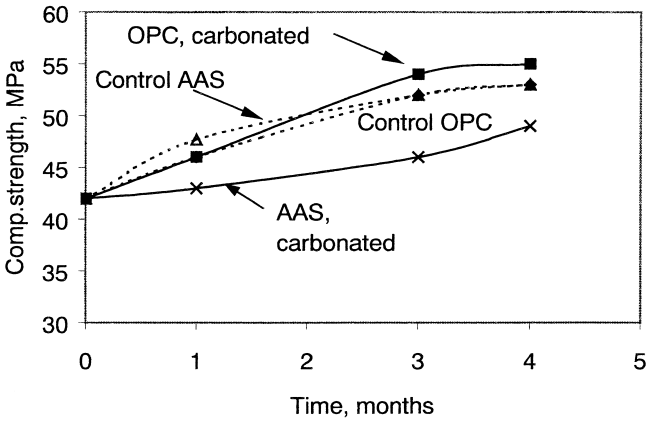

Fig. 3. Compressive strength of AAS and OPC concretes subjected to carbonation in air. The dotted curves show the compressive strength of AAS and OPC samples cured in water.

3. Results

AAS and OPC concrete specimens exposed to carbonation had no visible signs of deterioration, but some reduction in strength was measured in all AAS specimens. Fig. 1 shows the compressive strength evolution during immersion of the concrete in the 0.352-M solution of sodium bicarbonate that was used for simulation of carbonated ground water. Comparison of the strength reduction for AAS and OPC concrete in this experiment shows that AAS specimens had a higher strength reduction (10%) than OPC specimens (4%).

Fig. 2 presents the evolution of the depth of the carbonated layer in time for AAS and OPC concretes in this experiment. After 12 months of exposure to carbonated water, the depth of the layer having pH below 9 was 20 mm in AAS, and 12 mm in OPC concrete. Hence, pH

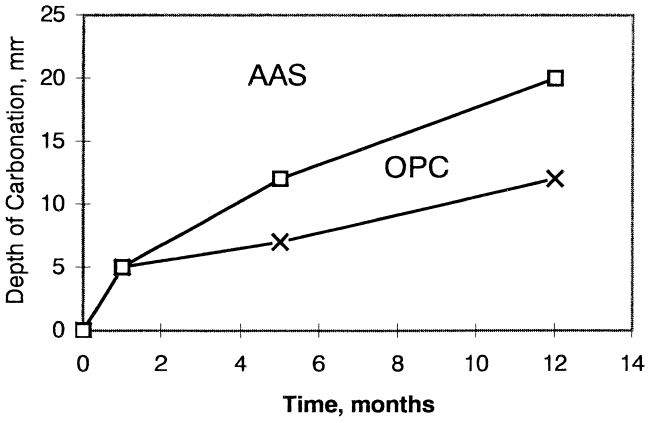

Fig. 2. Depth of carbonation in the 0.352-M solution of sodium bicarbonate.

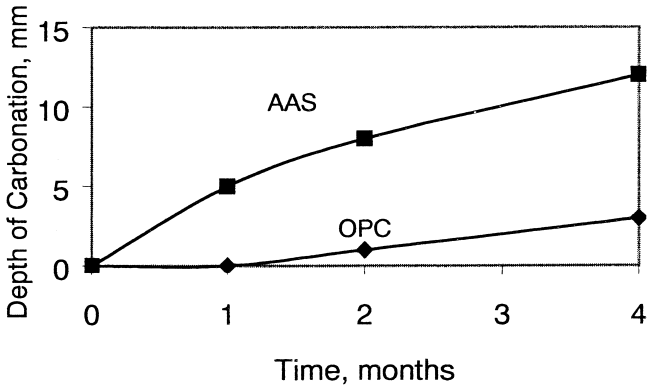

Fig. 4. Depth of carbonation in AAS and OPC concretes exposed to atmosphere containing 20% CO_2, 70% RH.

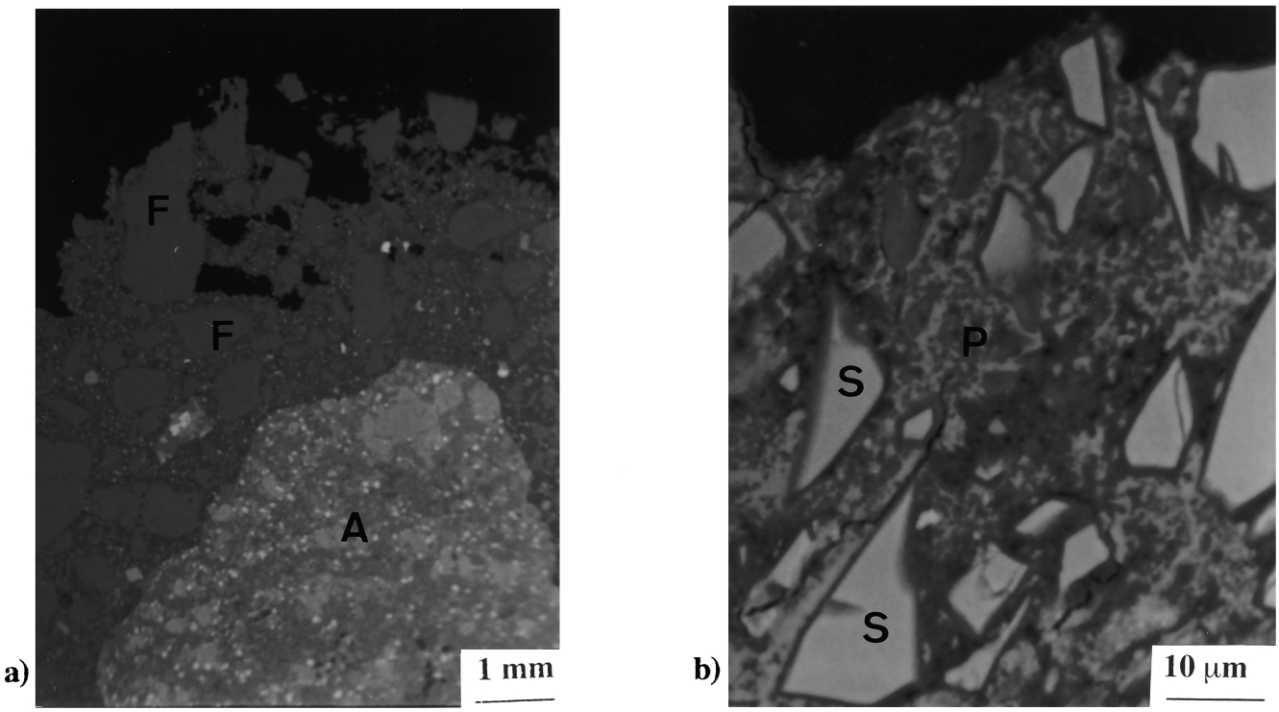

Fig. 5. (a–b) BEI of the surface area of AAS concrete exposed to carbonated solution (a = low magnification, b = high magnification). A = coarse aggregate, F = fine aggregate, P = paste, S = slag grain.

of the pore solution in AAS concrete decreased more rapidly than that in OPC concrete.

In the case of carbonation in air, CO_2 penetrates from the surface to the interior of concrete. Initially, carbonation in AAS developed mainly along shrinkage cracks occurring at the surface. The compressive strength evolution and the change in the pH of the concrete are shown in Figs. 3 and 4, respectively. Both strength reduction and carbonation depth were higher in AAS than in OPC concrete samples. OPC concrete samples had compressive strength increased in the experiment.

3.1. SEM and XRD

Two specimens of AAS concrete exposed to the carbonated solution were examined in SEM. The specimens were taken from the cross-section perpendicular to the surface exposed to deterioration. After exposure to the carbonated solution for 2 months, the AAS concrete specimen had some softening of the surface concrete layer. The AAS sample exposed to the carbonated solution for 4 months showed some loss of paste and aggregates from the surface (Fig. 5(a)) and left dark-grey and light-grey areas in the paste (Fig. 5(b)). The EDS analysis of the interior region in AAS paste revealed the presence of Ca, O, C, Si, Al and small amounts of Mg and Na. A summary of the individual EDS analyses of the AAS concrete samples exposed to carbonation and the control AAS concrete is presented as a plot Al/Ca vs. Si/Ca (Fig. 6).

Two specimens of AAS concrete exposed to atmosphere rich in CO_2 were examined by SEM. The microscopical investigation of AAS concrete showed that some new crystals appeared in the paste (Fig. 7(a–b)). For comparison, microstructure of a control AAS concrete sample is presented in Fig. 8. The new crystals formed from C-S-H and occupied a significant volume in the paste. EDS analysis of these crystals showed the presence of Ca, Si,

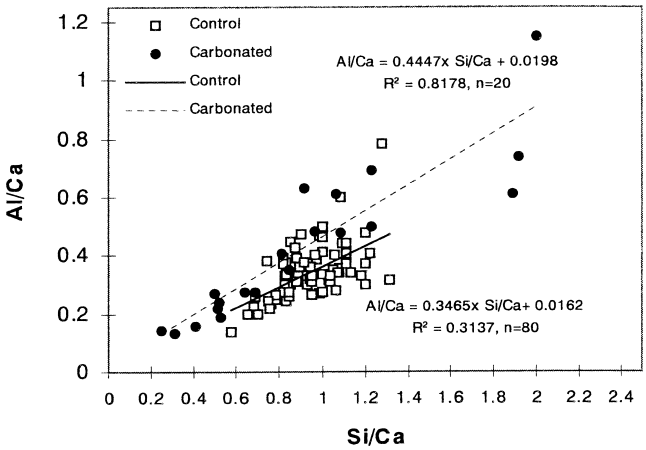

Fig. 6. Plot of Al/Ca vs. Si/Ca atom ratios from individual X-ray microanalyses for the control and exposed to carbonation AAS concretes.

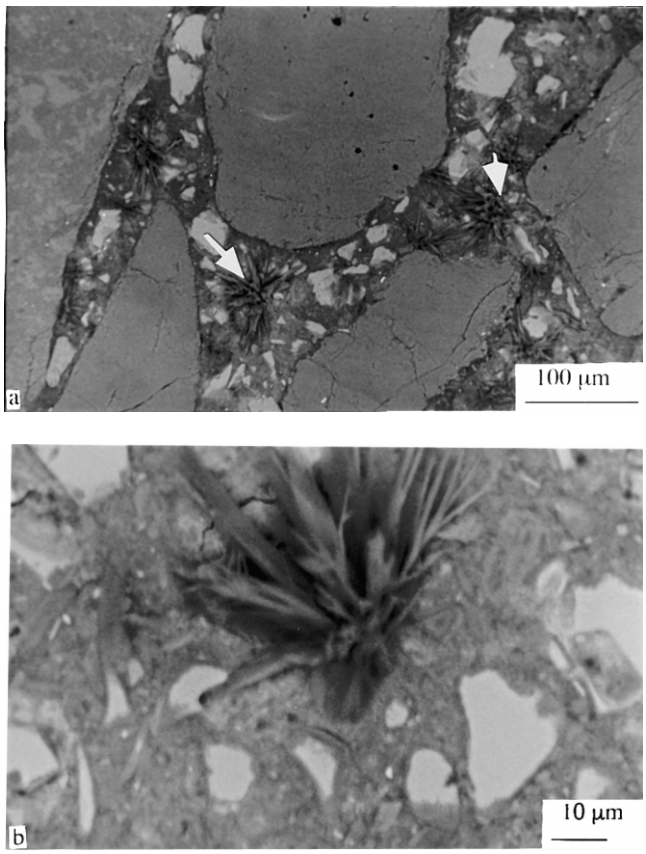

Fig. 7. BEI of the AAS concrete exposed to atmosphere rich in CO_2: (a) arrows show new crystals formed in carbonated AAS concrete; (b) enlarged new crystals in carbonated AAS concrete.

O, C and small amounts of Al, Mg, Na. Calcite was identified by XRD analysis in this concrete.

4. Discussion

In the experiments where concrete was immersed in the carbonated solution, it was found that on the concrete surface, the pH of AAS concrete was reduced to about 9

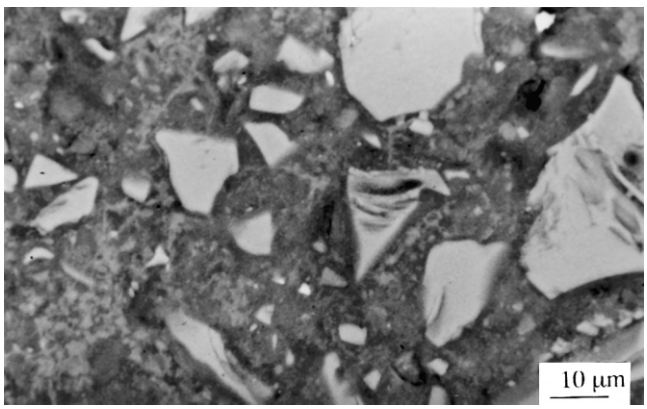

Fig. 8. BEI of the control sample of AAS concrete.

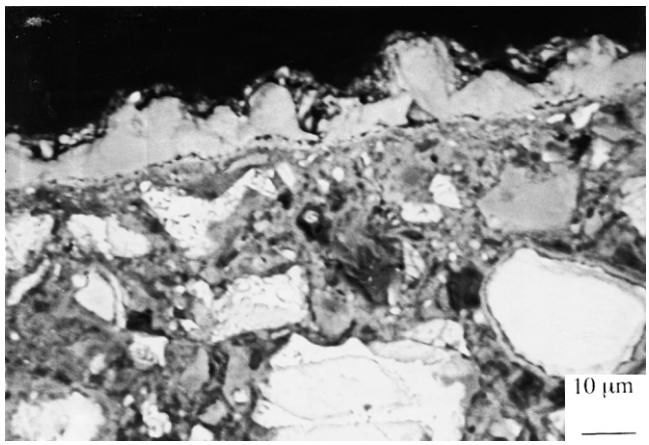

Fig. 9. BEI of the surface region in OPC concrete exposed to atmosphere rich in CO_2 for 2 months. Calcium carbonate (light grey) precipitated on the concrete surface created a barrier for further penetration of CO_2.

from its initial value of about 13.5. At meantime, a reduction in strength was also observed. The SEM examination indicated the formation of areas rich in Ca and C and the dark areas rich in Si and containing Al in the surface layer of the concrete. These areas possibly correspond to the decalcified C-S-H and calcium carbonate precipitates that had formed in the course of the carbonation reaction between slag paste and carbonate ions in the solution. The areas that contained considerable amounts of decalcified C-S-H and aluminosilicate gel became dark grey in SEM. Decalcified C-S-H and aluminosilicate gel caused concrete softening and some deterioration of strength was observed.

When AAS concrete was exposed to an atmosphere rich in CO_2, reduction in pH at the surface and crystallisation of calcite and decalcified C-S-H were also observed. In the areas of calcite crystallisation, an increased porosity was created (Fig. 7(a–b)). Thus, it is thought that due to carbonation the concrete diffusivity was probably increased, while the strength was decreased.

In both carbonation experiments in air and in solution, pH in the pore solution of slag concrete decreased more rapidly than in OPC concrete. Since Na is very soluble and is gradually lost from the AAS matrix when concrete is immersed in the solution, only Ca from C-S-H can buffer the pH in the pore solution. However, the calcium-to-silica ratio in C-S-H of AAS concrete is about 1, while for OPC concrete it is 1.7–2.0. Hence, AAS concrete has a low capacity to buffer the pH of the pore solution.

In both carbonation experiments, C-S-H in slag concrete was converted to calcite and decalcified C-S-H, which was rich in Si and contained Al. An increase in the Al/Si and Al/Ca ratios in some EDS analyses of the carbonated matrix was observed (Fig. 6), which is thought to be due to precipitation of calcium carbonate. It is likely that AlOH combines with SiOH groups on silica gel in products of carbonation and this produces an acid reaction. Previously, it was shown that the condensation of SiOH groups on silica

gel with AlOH groups leads to a formation of strong acid sites [10]. It was also demonstrated that there was a reaction between a fresh neutral silica sol and fresh neutral alumina sol, since a strong acid reaction then developed [11]. In the current investigation, the pH of the carbonated layer dropped to about 9–10, and a further decrease in the pH of the pore solution is possible due to carbonation. Therefore, the pH in AAS concrete may gradually decrease to 9–10 due to alkalis leaching into solution and/or carbonation. Thus, the test using phenolphtalein indicates a drop of the pH in AAS concrete due to both processes.

The carbonation in air and in solution starts from the concrete surface and penetrates slowly into the interior of the concrete. The speed-determining process is the diffusion of HCO_3^- and CO_2 into concrete, a process that obeys Fick's second law. By a rough estimation, the rate of carbonation (an increase of the carbonation depth with time) follows a square-root-time law. Thus, the pH curves have the parabolic shape.

The decisive parameter of concrete quality is permeability, which, for a given environment, depends on the pore structure. When AAS concrete is exposed to CO_2, C-S-H reacts producing calcium carbonate, decalcified C-S-H and aluminosilicate gel. Because in slag concrete the Ca content is low, deposits of $CaCO_3$ are rare. As a result of the carbonation reaction, porosity in the matrix may increase (Fig. 7). This increases the diffusivity of the concrete and the access of HCO_3^- and CO_2 to the interior. Therefore, the reaction front may proceed more rapidly inward. Thus, AAS concrete is probably more vulnerable to carbonation than OPC concrete.

It was observed that OPC paste is less vulnerable to carbonation. OPC paste contains more Ca than AAS paste in residue of C_3S and C_2S, CH and also in C-S-H phases. C-S-H has a Ca/Si ratio of about 1.7 and is in equilibrium with the pore solution of pH = 12.6–13.5. When OPC paste comes in contact with CO_2, calcium carbonate is formed, which has a low solubility, and when precipitated in pores, the diffusivity of the matrix further decreases. Thus, in OPC paste, a dense surface layer rich in calcium carbonate is created due to carbonation (Fig. 9). Precipitated calcium carbonate in the surface layers of OPC paste forms a barrier for diffusion, while porosity in the interior regions may have increased [12]. This barrier limits the access of CO_2 into the interior. The rate of carbonation reaction declines and thus, further carbonation in OPC paste progresses slowly.

Previously, Byfors et al. [13] and Pu et al. [2] also reported higher carbonation rates in AAS than in OPC concrete. Pu et al. [2] showed that in an atmosphere containing 20% CO_2 at 70% relative humidity, loss of strength was significant for low strength concrete, and much less in high strength concrete. The depth of carbonation also depended on the strength of concrete, and it varied from 2 (80 MPa) to 40 mm (20 MPa). Thus, carbonation of the concrete with a high initial strength (80 MPa) was very small compared to that of concrete with a low initial strength (20 MPa). It is possible that the difference in the carbonation rates between concretes was due to high porosity of the microstructure of the concrete with low strength. From the experimental data of carbonation depth for the AAS concrete with w/b ratio 0.36 and compressive strength 66 MPa exposed to outdoor conditions, Byfors et al. [13] estimated that reinforcement with a 30-mm AAS concrete cover could start corroding after a lapse of 60 years.

In the present investigation, there was some increase in the strength of AAS concrete throughout the exposure to carbonated solution and an atmosphere high in carbon dioxide (with an initial strength of 40 MPa). The depth of partially carbonated zone in the solution was about 20 mm and in the atmosphere it was about 12 mm. Initially, carbonation in AAS occurred mainly along shrinkage cracks developed on the surface. The rate of carbonation in AAS was clearly higher than that in OPC concrete.

5. Conclusions

The investigation of resistance of AAS concrete to carbonation examined the performance of AAS concrete in two carbonation tests. It was found that AAS concrete of Grade 40 had lower resistance to carbonation than that of OPC concrete.

Acknowledgments

The financial support for this project was provided by Independent Cement and Lime, Blue Circle Southern Cement and Australian Steel Mill Services. The efforts and assistance with the laboratory work provided by Jeff Doddrell, Roger Doulis and Peter Dunbar are also gratefully acknowledged.

References

[1] D.M. Roy, G.M. Idorn, Hydration, structure, and properties of blast furnace slag cements, mortars, and concrete, ACI J. 79 (12) (1982) 444–457.
[2] X.C. Pu, C.C. Gan, S.D. Wang, C.H. Yang, Summary Reports of Research on Alkali-Activated Slag Cement and Concrete, vols. 1–6, Chongqing Institute of Architecture and Engineering, Chongqing, 1988.
[3] V.D. Glukhovsky, Slag-Alkali Concretes Produced from Fine-Grained Aggregate, Vishcha Shkola, Kiev, USSR, 1981 (in Russian).
[4] V.D. Glukhovsky, V.A. Pakhomov, Slag-Alkali Cements and Concretes, Budivelnik Publishers, Kiev, 1978 (in Russian).
[5] G.W. Groves, D.I. Rodway, I.G. Richardson, The carbonation of hardened cement pastes, Adv. Cem. Res. 3 (11) (1990) 117–125.
[6] I.G. Richardson, G.W. Groves, A.R. Brough, C.M. Dobson, Structural changes due to carbonation in hardened cement paste, Proceedings of the 9th International Congress on the Chemistry of Cement, National Council for Cement and Building Materials, New Delhi, 1992, pp. 298–303.
[7] G.W. Groves, A.R. Brough, I.G. Richardson, C.M. Dobson, Progres-

sive changes in the structure of hardened C_3S cement pastes due to carbonation, J. Am. Ceram. Soc. 74 (11) (1991) 2891–2896.
[8] L.J. Parrott, D.C. Killoh, Carbonation in a 36 year old, in-situ concrete, Cem. Concr. Res. 19 (4) (1989) 649–656.
[9] L.J. Parrott, A review of carbonation in reinforced concrete, Cement and Concrete Assoc. Report C/1-0987, 1987, p. 126.
[10] M.W. Tamele, Chemistry of the surface and the activity of alumina–silica cracking catalyst, Discuss. Faraday Soc. 8 (1950) 270–274 (Heterog. Catal.).
[11] R.K. Iller, The Colloidal Chemistry of Silica and Silicates, Cornell Univ. Press, Ithaca, NY, 1955, p. 261.
[12] Th.A. Bier, Influence of type of cement and curing on carbonation process and pore structure of hydrated cement pastes, in: L.J. Struble, Th.A. Bier, P.W. Brown (Eds.), Microstructural Development During Hydration of Cement, Proc. Mater. Res. Soc. Symp. 85 (1987) 123–134.
[13] K. Byfors, G. Klingstedt, V. Lehtonen, H. Pyy, L. Romben, Durability of concrete made with alkali-activated slag, in: V.M. Malhota (Ed.), Fly Ash, Silica Fume, Slag and Natural Pozzolans in Concrete, Proceedings 3rd CANMET/ACI Inter. Conf., Trondheim, Norway, ACI: Detroit, ACI SP-114, vol. 2 1989, pp. 1429–1466.